

Co-solvent Assisted Spray Pyrolysis for the Generation of Metal Particles

Jung Hyeun Kim*, Valeri I. Babushok**, Thomas A. Germer[†], George W. Mulholland** and Sheryl H. Ehrman*^{a)}

*Department of Chemical Engineering
University of Maryland
College Park, Maryland 20742

**Fire Research Division
National Institute of Standards and Technology
Gaithersburg, Maryland 20899

[†]Optical Technology Division
National Institute of Standards and Technology
Gaithersburg, Maryland 20899

^{a)} Corresponding author, e-mail: sehrman@eng.umd.edu; tel: (301) 405-1917

Abstract: A co-solvent assisted spray pyrolysis process was developed for the formation of phase pure metal particles from metal salt precursors without the direct addition of hydrogen or other reducing gas. Generation of phase pure copper and nickel particles from aqueous solutions of copper acetate, copper nitrate, and nickel nitrate over the temperature range of 450 °C to 1000 °C was demonstrated. Addition of ethanol as a co-solvent plays a crucial role in producing phase pure metal powders. Results of a modeling study of ethanol decomposition kinetics suggest that co-solvent decomposition creates a strong reducing atmosphere during spray pyrolysis via *in-situ* production of hydrogen and carbon monoxide.

I. INTRODUCTION

Micro or nanometer size metal particles have various applications such as electrode materials for electronic products,¹ electromagnetic interference (EMI) shielding materials for electronic packaging,² and catalysts for synthesizing carbon nanotubes.³ Spray pyrolysis is a useful tool for large-scale or small-scale production of particles with controlled particle size because the final product properties can be controlled through the choice of precursor and solution concentration or by changing aerosol decomposition parameters. Generally, in a spray pyrolysis process, reaction temperature and carrier gas composition are basic operating variables. In addition, solution properties such as precursor composition, concentration, or the addition of a co-solvent may be crucial to achieve the desired product composition and morphology. For example, morphological variation of magnesium oxide particles produced by the evaporative decomposition technique from three different precursors, magnesium chloride, magnesium acetate, and magnesium nitrate, was reported.⁴

Preparation of metal particles by spray pyrolysis of metal salts is especially challenging. In chemical vapor deposition (CVD) of metals, the decomposition of the organic ligand may, such as in the case of the CVD of copper from bis(hexafluoroacetylacetonate)copper(II) [Cu(hfac)₂],

create a reducing environment at the surface resulting in the deposition of pure metal from a precursor containing metal in an oxidized form.⁵ In spray pyrolysis, however, both surface and solid-state chemical reactions occur during the conversion from precursor to product particle. For the metal salt precursors commonly used in spray pyrolysis processes, decomposition of the anion does not typically result in pure metal particle formation. Additional measures that have been taken include the addition of reducing gases such as hydrogen and carbon monoxide for copper⁶ and nickel⁷ production, and addition of aqueous ammonium for production of pure metallic nickel.⁸

Size-monodisperse nanoparticles can be obtained using an electrostatic classifier downstream of the spray pyrolysis generator to select particles of the desired size. In a previous paper,⁹ we describe the electrostatic classification method for producing size-monodisperse metal nanoparticles for use as size standards in semiconductor metrology via hydrogen free spray pyrolysis of copper nitrate at 600 °C with an ethanol co-solvent.

In this paper, results are presented for copper particle formation from copper acetate and nitrate precursors with an ethanol co-solvent, and for nickel formation from nickel nitrate with the same co-solvent. The effects of co-solvent, precursor, and reaction temperature on the final product composition were investigated. Results demonstrate that the use of a co-solvent in preparation of metal particles by spray pyrolysis is a convenient, economical, and easily implemented technique. Model calculations of co-solvent decomposition kinetics, and calculations to determine the equilibrium phase diagram of the copper-oxygen system were performed to examine the role of the co-solvent in the pyrolysis reactor.

II. EXPERIMENTAL

A. Particle generation

Precursor solutions (0.30 mol/L) were prepared from three different metal salt precursors: copper nitrate [Cu (NO₃)₂·2.5H₂O], copper acetate [Cu (CH₃COO)₂·H₂O], and nickel nitrate [Ni (NO₃)₂·6H₂O]. All chemicals are reagent grade and were used without further purification. Deionized water was used for all solutions. For the co-solvent solutions, a 10 % volume fraction of ethanol solution was made prior to adding metal precursors. All solutions were stirred for at least 3 hours using a magnetic stirrer. A spray pyrolysis system was used in this study, consisting of particle generation, classification, and collection units. A precursor solution consisting of metal salts dissolved in either pure water or a mixture of water and co-solvent is atomized with a Retec¹⁰ type nebulizer using nitrogen gas supplied at a constant pressure of 1.4×10^5 N m⁻². The pressure at the reactor inlet after the nebulizer was 27 N m⁻² above atmospheric pressure. The volume mean diameter and geometric standard deviation of the droplets produced by the nebulizer are 5.1 μm and 2.0 respectively.¹¹ The nebulized solution droplets, suspended by nitrogen carrier gas, are then carried into the high temperature reactor furnace where droplets evolve into final product particles by solvent evaporation and precursor decomposition. The precursor solution was delivered with a rate of 0.006 cm³s⁻¹ (20 mL h⁻¹), and the nitrogen carrier gas flow rate was 83 cm³ s⁻¹ (5 L min⁻¹). The reactor consisted of a quartz tube, 2.54 cm diameter and 76.2 cm length, heated by two horizontal furnaces in series (both Lindberg, type 55035). The furnace set point temperature for these experiments was varied between 300 °C and 1000 °C. Temperature profiles along the centerline of the quartz tube were measured using a type K thermocouple, and examples are shown in Fig. 1. For the measurements of particle size distributions, a differential mobility analyzer (TSI, Inc., Model 3071) and a condensation nucleus

counter (TSI, Inc. Model 3022A) were used. Detailed descriptions of the size classification system can be found elsewhere.⁹

B. Characterization

X-ray diffraction (XRD) patterns and Fourier transformed infrared (FTIR) spectroscopy were used for composition analysis, and scanning electron microscopy (SEM) was used for particle morphology characterization. Powder was collected by filtration immediately downstream of the furnace for XRD and FTIR analysis. XRD measurements were performed using a Philips PW 1800 diffractometer with a graphite monochromator and $\text{CuK}\alpha$ radiation. For the XRD measurements, first a suspension of the collected particles in methanol was formed, and then the suspension was dispersed dropwise onto an amorphous glass microscope slide to make a thick film via solvent evaporation. Data analysis of XRD spectra was performed using Jade 6.0 software from MDI. For FTIR spectroscopy analysis, the collected powders were combined with KBr in the mass ratio of 1:50 (powder:KBr), and made into pellets. A Magna 550 IR spectrometer system was used for the measurements. SEM images of powders were obtained using a Hitachi S-4500 Field Emission SEM, and powder films were prepared in the same fashion as above for XRD using silicon wafers as the substrate. SEM images were used to observe the surface morphology of particles formed at different reaction temperatures.

III. MODEL DEVELOPMENT

Model calculations of the ethanol co-solvent decomposition were performed to investigate the influence of decomposition products on the metal particle formation. For the ethanol decomposition study, Marinov's¹² kinetic model consisting of 389 reversible elementary reactions with 63 species was used with the following modifications. Rate constants of three decomposition reactions ($\text{C}_2\text{H}_5\text{OH} = \text{CH}_3 + \text{CH}_2\text{OH}$, $\text{C}_2\text{H}_5\text{OH} = \text{C}_2\text{H}_5 + \text{OH}$, and $\text{C}_2\text{H}_5\text{OH} = \text{C}_2\text{H}_4 + \text{H}_2\text{O}$) were modified in accord with the recent work of Tsang.¹³ In addition, the $\text{C}_2\text{H}_5\text{OH} + \text{O}_2 = \text{C}_2\text{H}_4\text{OH} + \text{HO}_2$ reaction having the pre-exponential factor of $4 \times 10^{10} \text{ L mol}^{-1} \text{ s}^{-1}$ and the activation energy of 188 kJ mol^{-1} was included in the kinetic model because this low temperature initiation reaction is important for ethanol decomposition in the presence of oxygen at temperatures below $800 \text{ }^\circ\text{C}$.¹⁴ The possibility of heterogeneous reactions was considered but thought to be relatively unimportant for our experimental temperature ranges,¹⁴ so only gas phase reactions were included in the model. The kinetics of the co-solvent decomposition reactions were simulated with the CHEMKIN-II software package.¹⁵ For generation of the equilibrium phase diagram of the copper-oxygen system, thermodynamic data of copper compounds were taken from the database of Gurvich *et al.*¹⁶

IV. RESULTS AND DISCUSSION

Fig. 2 shows the XRD patterns obtained from 0.30 mol/L solutions of copper nitrate and acetate precursors dissolved in deionized water. Phase pure copper particles can be produced at temperatures above $600 \text{ }^\circ\text{C}$ from copper acetate as shown in Fig. 2a; however, it is impossible to obtain pure copper from copper nitrate (Fig. 2b) even at temperatures as high as $1000 \text{ }^\circ\text{C}$. Although the decomposition products are all mixtures of copper and copper oxide, the intensity of the oxide peaks of the products decreases with increasing temperature as shown in the nitrate decomposition. The solubility of copper acetate ($7.2 \text{ g}/100 \text{ cm}^3$ water) is much lower than that of

nitrate (130 g/100 cm³ water).¹⁷ Therefore, copper nitrate should be considered as the more suitable precursor if large-scale production or production of larger particles is desired. Fig. 3 shows the XRD results for the 0.30 mol/L copper precursors with 10 % volume fraction of ethanol as a co-solvent. With the co-solvent, phase pure copper particles are obtained even from copper nitrate precursor (Fig. 3b) at temperatures above 600 °C. Moreover, use of copper acetate precursor (Fig. 3a) results in phase pure copper even at a lower temperature of 450 °C compared to 600 °C without a co-solvent. In Fig. 2 and 3, some unidentified peaks (at $2\theta = 13^\circ$ and 26°) can be seen for copper nitrate products produced at 300 °C. These may be attributable to un-decomposed nitrate precursor or to its partial decomposition products.

FTIR spectra obtained from the copper acetate and nitrate decomposition at 300 °C and from the copper nitrate without adding co-solvent at four different decomposition temperatures are shown in Fig. 4a and b. The strong band, from 1300 cm⁻¹ to 1420 cm⁻¹, observed in the IR spectrum of powder produced from copper nitrate at 300 °C is assigned to the un-decomposed nitrate group.¹⁸ From Fig. 4a, two different copper oxide peaks indicate the importance of precursor composition. Copper nitrate decomposition produces tenorite (CuO) as a primary low temperature product indicated by the peak at 500 cm⁻¹, but copper acetate produces cuprite (Cu₂O) as a primary product shown by the peak at 620 cm⁻¹.¹⁹ In addition, the temperature effect on the reduction of copper oxide produced from copper nitrate decomposition can be seen in Fig. 4b. At the higher reaction temperature, the copper oxide compounds are more strongly reduced, from tenorite to cuprite. This observation will be discussed later in the context of an equilibrium phase diagram of the copper-oxygen system.

Fig. 5 shows the morphology of copper particles generated at 600 °C, and at 1000 °C using copper nitrate precursor at a concentration of 0.30 mol/L with 10 % ethanol co-solvent. As shown in Fig. 5a, the copper powder sample formed at 600 °C contains some hollow particles, but if formed at 1000 °C, no hollow particles are visible in the sample. However, Lenggoro *et al.*²⁰ demonstrated experimentally that hollow zirconia particles are formed if the reactor temperature is high. This result corresponded to their simulation results. We believe that longer residence time, higher precursor solution concentration, and smaller droplets in the spray pyrolysis process described here help to form denser particles. In addition, for metal particle formation, high reaction temperature closes to the metal melting point (1080 °C for copper) may help to form dense particles by a melting process. The density of copper powder produced at lower temperature is likely less dense, indicative of some hollow or porous particles as shown in Fig 5a. Furthermore, the ethanol co-solvent may promote the evaporation of ethanol/water solvent mixture. In addition, the solubility of precursor decreases by adding ethanol co-solvent, and it may help to form dense particles by decreasing equilibrium saturation concentration compared to the pure water case, as described Lenggoro *et al.*²⁰ for ZrO₂ particles. Resultant particle size distributions are shown in Fig. 6. Copper and nickel particles produced from copper nitrate and nickel nitrate precursors at 900 °C show similar size distributions since the same nebulizer and precursor solution concentrations were used, and because the molar volumes of the two metals are similar. Our size distribution measurements are reported for particle diameters up to 300 nm, because of limitations associated with the DMA, as described elsewhere^{9,21}.

X-ray diffraction patterns of nickel particles from nickel nitrate 0.30 mol/L solutions at various temperatures and amounts of ethanol co-solvent are shown in Fig. 7. Trends similar to those seen for copper particles (Fig. 3) were observed. However, higher temperatures and a greater concentration of co-solvent, 30 % volume fraction of ethanol in water, were required in order to obtain phase pure nickel products, likely because nickel oxide has higher bond energy

than that of copper oxide. According to these results, it is clear that the reduction process is more favorable at higher reaction temperatures and with a higher concentration of co-solvent.

The results of product composition for all copper and nickel experiments are summarized in Table I.

A. Effect of co-solvent

As explained above, the effect of adding the co-solvent is to reduce the temperature required to obtain phase pure copper starting from copper acetate, and to enable the production of phase pure copper from copper nitrate and nickel from nickel nitrate. These findings are attributed to the strong reducing conditions created by co-solvent decomposition. In previously reported studies, pure copper⁶ and nickel⁷ particles were produced using a mixture of hydrogen and nitrogen gases in a pyrolysis reactor. In those cases, hydrogen gas played a significant role in reducing the oxide products that result from the oxygen impurities and by-products into pure metals. In those processes, though, the concentration required to reduce the metal oxide particles is greater than the flammability limit of hydrogen in air, resulting in a potential safety problem. The use of a co-solvent as a reducing agent accomplishes the same role under safer conditions.

Recently, metal nanoparticles of Ag, Au, Pd, Ru, and Cu were produced by the solution phase reduction of their salts by alcohol under refluxing conditions,^{22,23} and pure nickel particles were produced in the gas phase from NiCl with the aid of aqueous ammonium⁸ and from nickel formate with formic acid²⁴ as co-solvents without using reducing gas. In those cases, alcohol, ammonium, and formic acid play crucial roles either by reducing metal oxides or by preventing oxide formation in solution phase or gas phase.

In this study, experimental results demonstrate that the use of ethanol as a co-solvent decreases the operating temperature required to obtain phase pure copper and nickel powders. Fig. 8 shows gaseous products from the kinetic modeling of homogeneous ethanol decomposition at 1000 °C. At temperatures below 600 °C, complete decomposition could not be achieved during a 1.5-second residence time, the minimum residence time for our experiments. As can be seen in Fig. 8, hydrogen, carbon monoxide, and carbon dioxide were produced as gaseous final products with acetaldehyde, ethylene, and ethane as intermediate species. This implies that reducing agents such as hydrogen and carbon monoxide create a strongly reducing atmosphere by consuming oxygen from oxygen impurities or by-products of precursor decomposition. A note should be made here to compare the level of hydrogen produced *in-situ* from the co-solvent decomposition, to that added in processes developed by other researchers.^{6,7} The resulting hydrogen concentration from ethanol decomposition is estimated to be approximately several thousand ppm, while its amount increases an order of magnitude if hydrogen gas is added directly. Thus, it appears that the use of a co-solvent to create reducing conditions inside the reactor is much more efficient than direct use of hydrogen gas for metal production, and it results in safer operating conditions.

Fig. 9 shows the temperature dependency of hydrogen yield with different initial oxygen concentrations for a 1.5-second residence time. The presence of a small amount (0.1 ppm) of oxygen increases hydrogen yield by several orders of magnitude. This is due to the lower activation energy of the initiation reaction ($C_2H_5OH + O_2 = C_2H_4OH + HO_2$) compared to that of the homogeneous ethanol decomposition reaction,¹² and due to an increased amount of radicals. The role of oxygen is to initiate ethanol decomposition and to increase the rate of the initial reaction step, and thus the presence of oxygen reduces the induction period and the decomposition temperature. Without oxygen impurities, the decomposition temperature to obtain

a steady-state concentration of hydrogen from the ethanol decomposition is about 800 °C, while the temperature markedly decreases to about 600 °C if several tens of ppm of oxygen are present.

Oxygen sources in our experimental system are oxygen dissolved in water and in the co-solvent, impurities in carrier gas (N_2), and oxygen produced from precursor decomposition as shown in Table II. Nitrate decomposition produces a half mole of oxygen from each mole of precursor.²⁷ We estimate the amount of oxygen in our process is approximately 20 ppm if there are no oxygen by-products from precursor decomposition, and it is approximately 170 ppm if a nitrate precursor is used (Table II). If a small amount of oxygen is present, the ethanol decomposition temperature corresponds to the experimental temperature at which phase pure copper was produced from copper nitrate precursor (Fig. 3). The sensitivity of ethanol decomposition to oxygen disappears above a few hundred-ppm level of oxygen. If the oxygen content exceeds about 2000 ~ 4000 ppm, hydrogen concentration decreases because it will combine with oxygen to form water. At this oxygen concentration, the level of hydrogen produced is comparable with the oxygen concentration, and the reaction mode changes from decomposition to ethanol oxidation.

B. Effect of precursor

The composition of the metal salt precursor affects the phase of the material produced. Subject to slow (10–20 °C/min) heating rates in a thermo-gravimetric study, copper acetate produces Cu metal under nitrogen flow, while it reacts to form CuO as a final product under an atmosphere of air.²⁸⁻³¹ This implies that the decomposition of copper acetate is strongly affected by the ambient atmosphere. The decomposition of copper nitrate yields CuO even in a nitrogen atmosphere,^{32,33} and this may be attributable to the reaction with oxygen formed as a by-product during decomposition. Nickel nitrate decomposition also produces NiO as a final product under a nitrogen atmosphere.³²

In this study, if copper acetate was used, rather than copper nitrate, phase pure copper was obtained at temperatures higher than 600 °C, without addition of any co-solvent. However, copper acetate is less soluble than copper nitrate in water, so the use of copper nitrate as a precursor would be more desirable for industrial applications. Even when a co-solvent was used, copper nitrate and copper acetate showed different decomposition products at temperatures less than 600 °C. Copper nitrate, which may produce a higher concentration of oxygen during precursor decomposition than copper acetate (see Table 2), gives CuO as a primary low temperature product, but copper acetate gives Cu_2O as a major product with small amount of Cu in the crystalline phase. This composition difference suggests a strong dependency on the concentration of oxygen. These results will be further discussed in the context of the phase equilibria for this system.

C. Effect of temperature

In addition to the effects of co-solvent and precursors, reaction temperature determines the final products of metal precursor decomposition in spray pyrolysis. Fig. 10 shows the equilibrium phase diagram of the copper-oxygen system at atmospheric pressure as a function of oxygen concentration and temperature. Experimentally measured product compositions are close to the calculated equilibrium products. For example, if the amount of oxygen is about 170 ppm (Table II) corresponding to the use of copper nitrate precursor, the predicted phase for temperatures less than 600 °C is CuO, just above the CuO/ Cu_2O boundary line. The change of product composition from tenorite to cuprite with an increased reaction temperature was already

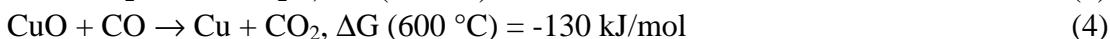
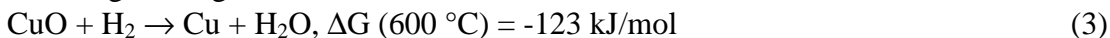
observed in the XRD and IR results. At higher reaction temperatures, reduced copper compounds are thermodynamically favored, and phase pure copper is formed at temperatures higher than 1300 °C. On the other hand, if the oxygen concentration is about 20 ppm (Table II) as expected with the use of copper acetate, the equilibrium phase composition would be a Cu₂O/Cu mixture just below the boundary line of CuO/Cu₂O. Correspondingly, we observe Cu₂O as a major phase formed with Cu as a minor phase as shown in Fig. 2a for temperatures less than 450 °C. Furthermore, phase pure copper was obtained at an increased reaction temperature as estimated in Fig. 10. From the analysis of the phase diagram, experimental conditions for the generation of phase pure copper particles can be predicted, incorporating chemical reaction effects of reducing agents as explained in the following section.

D. Suggested reaction mechanisms

From analysis of the precursor and co-solvent effects, a mechanism for pure copper particle formation from the decomposition of two copper precursors can be suggested. For copper nitrate, nitrate decomposition produces oxygen leading to formation of CuO. The following reactions have been suggested by other researchers for copper nitrate decomposition during spray pyrolysis under a nitrogen atmosphere.²⁷

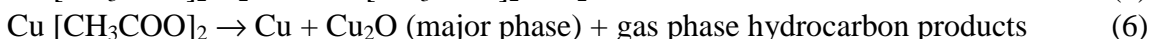


It is believed that CuO is further reduced to phase pure copper under the highly reducing atmosphere created from ethanol decomposition at temperatures above 600 °C, Eqs. 3 and 4. The estimated amount of hydrogen and carbon monoxide formed from ethanol decomposition is an order of magnitude greater than the amount of CuO on a molar basis.

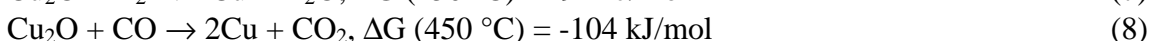


Furthermore, (3) and (4) are spontaneous reactions with negative changes in Gibbs free energy.³⁴ If there is no reducing agent present, higher temperatures thermodynamically favor reduction of CuO into a mixture of Cu₂O and Cu (Fig. 10).

If copper acetate precursor is used, oxygen is present from impurities, but only at a level of several tens of ppm (Table II). In addition, acetate decomposition does not produce oxygen, but rather several hydrocarbon components. Thus, a Cu₂O/Cu mixture with Cu₂O as the major phase is formed at temperatures around 300 °C in the presence of oxygen impurities as discussed previously. A copper acetate decomposition reaction is suggested as equation 6, following a dehydration step of equation 5 reported elsewhere.³⁰



Without a co-solvent, phase pure copper was produced at 600 °C or above, but the temperature required to obtain phase pure copper decreases down to 450 °C if a co-solvent is used. We attribute this to the consumption of the small amount of remaining impurity by hydrogen and carbon monoxide at 450 °C. Otherwise, the remaining impurity oxygen may help to form a small fraction of cuprite as seen in Fig. 2a. Thus, the cuprite phase is reduced into phase pure copper as shown below.



Also, (7) and (8) are spontaneous reactions with negative changes in Gibbs free energy at 450 °C.³⁴ If there is no reducing agent, the Cu₂O phase is thermodynamically favored to form

pure Cu as reaction temperatures increase in accord with the equilibrium phase diagram (Fig. 10).

The mechanism of nickel formation from nickel nitrate is analogous to that for copper formation from copper nitrate. The NiO phase was formed as a primary product without a co-solvent as shown in Fig. 7, the same result as reported by other researchers.³² If the co-solvent is added, phase pure nickel is formed by reaction with the reducing agents formed during ethanol decomposition.

V. CONCLUSIONS

Generation of phase pure copper and nickel particles was demonstrated via spray pyrolysis of copper acetate, copper nitrate, and nickel nitrate in the temperature range between 300 °C and 1000 °C. Phase pure copper powder was generated from copper nitrate precursor with 10 % volume fraction of ethanol at temperature above 600 °C, and from copper acetate precursor with 10 % volume fraction of ethanol at temperature above 450 °C. Phase pure nickel powder was produced from nickel nitrate precursor with 30 % volume fraction of ethanol at temperature above 900 °C. The addition of co-solvent, selection of precursors, and reaction temperature in spray pyrolysis were the main factors in determining final product composition. Results of a study of ethanol decomposition kinetics suggest that a highly reducing atmosphere was achieved during copper and nickel particle synthesis, via *in-situ* production of hydrogen and carbon monoxide. Interestingly, the presence of a small amount (< 300 ppm) of oxygen appears to increase hydrogen yield from ethanol decomposition, and thus may aid in formation of metal particles.

ACKNOWLEDGEMENTS

Authors would like to acknowledge Mr. Eric B. Steel for help with X-ray diffraction measurements and Dr. John Small for assistance with SEM images. We also thank Dr. A.G. Nasibulin for helpful discussions regarding phase diagrams of copper compounds.

REFERENCES

1. W. Chen, L. Li, J. Qi, Y. Wang, and Z. Gui, *J. Am. Ceram. Soc.* **81**, 2751 (1998).
2. V. Brusic, G. S. Frankel, J. Roldan, and R. Saraf, *J. Electrochem. Soc.* **142**, 2591 (1995).
3. Y. Li, J. Liu, Y. Wang, and Z. L. Wang, *Chem. Mater.* **13**, 1008 (2001).
4. T. J. Gardner and G. L. Messing, *Thermochimica Acta* **78**, 17 (1984).
5. T. T. Kodas and M. J. Hampden-Smith, *The Chemistry of Metal CVD*, (VCH Publishers Inc., New York, 1994), Chapter 4–5.
6. D. Majumdar, T. Shefelbine, T. Kodas, and H. Glicksman, *J. Mater. Res.* **11**, 2861 (1996).
7. K. Nagashima, M. Wada, and A. Kato, *J. Mater. Res.* **5**, 2828 (1990).
8. B. Xia, I. W. Lenggoro, and K. Okuyama, *J. Mater. Res.* **15**, 2157 (2000).
9. J. H. Kim, T. A. Germer, G. W. Mulholland, and S. H. Ehrman, *Adv. Mater.* **14**, 518 (2002).
10. Certain commercial equipment, instruments, or materials are identified in this paper in order to specify the experimental procedure adequately. Such identification is not intended to imply recommendation or endorsement by the National Institute of Standards and Technology, nor is it intended to imply that the materials or equipment identified are necessarily the best available for the purpose.

11. B. Y. H. Liu, *Fine Particles: Aerosol Generation, Measurement, Sampling, and Analysis*, (Academic Press, New York, 1976), Chapter 4, pp. 74.
12. N. M. Marinov, *Int. J. Chem. Kinet.* **31**, 183 (1999).
13. W. Tsang, *Proceedings of the Second Joint Meeting of the US Sections of the Combustion Institute*, Paper 92, (Oakland, CA, March 2001).
14. C. H. Bamford and C. F. H. Tipper, *Gas Phase Combustion: Comprehensive Chemical Kinetics*, (Elsevier Scientific Publishing Company, **Vol 17**, 1977).
15. R. J. Kee, F. M. Rupley, and J. A. Miller, *CHEMKIN-II: A Fortran Chemical Kinetics Package for the Analysis of Gas Phase Chemical Kinetics*, (Sandia National Laboratory, SAND 89-8009B, 1989).
16. L. V. Gurvich, V. S. Iorish, D. V. Chekhovskoi, A. D. Ivanisov, A. Yu. Proskurnev, V. S. Yungman, V. A. Veits, and G. A. Bergman, *IVTANTHERMO – Database of Thermodynamic Properties of Individual Substances*, Institute of High Temperatures, Moscow, 1993.
17. D. R. Lide, *CRC Handbook of Chemistry and Physics*, (CRC Press, USA, **74th** Edition, 1992).
18. M. K. Wilson, in *Determination of organic structures by physical methods*, edited by F. C. Nachod and W. D. Phillips, (Academic Press, New York, 1962), **Vol. 2**, Chapter 3, pp. 181.
19. J. R. Ferraro and L. J. Basile, *Fourier Transform Infrared Spectroscopy: applications to chemical systems*, (Academic Press, New York, 1978), **Vol. 1**, Chapter 3, pp. 127.
20. I. W. Lenggoro, T. Hata, F. Iskandar, M. M. Lunden, and K. Okuyama, *J. Mater. Res.* **15**, 733 (2000).
21. P. D. Kinney, D. Y. H. Pui, G. W. Mulholland, and N. P. Bryner, *J. Res. Natl. Inst. Stand. Technol.* **96**, 147 (1991).
22. S. Ayyappan, R. S. Gopalan, G. N. Subbanna, and C. N. R. Rao, *J. Mater. Res.* **12**, 398 (1997).
23. F. Bonet, V. Delmas, S. Grugeon, R. H. Urbina, P-Y. Silvert, and K. Tekaiia-Elhsissen, *Nanostructured Mater.* **11**, 1277 (1999).
24. B. Xia, I. W. Lenggoro, and K. Okuyama, *J. Am. Ceram. Soc.* **84**, 1425 (2001).
25. D. Tromans, *Ind. Eng. Chem. Res.* **39**, 805 (2000).
26. I. Kutsche, G. Gildehaus, D. Schuller, and A. Schumpe, *J. Chem. Eng. Data* **29**, 286 (1984).
27. K. Nagashima, T. Iwaida, H. Sasaki, Y. Katatae, and A. Kato, *Nippon Kagaku Zasshi* **1**, 17 (1990).
28. J. Maslowska and A. Baranowska, *J. Thermal Anal.* **29**, 309 (1984).
29. M. Afzal, P. K. Butt, and H. Ahmad, *J. Thermal Anal.* **37**, 1015 (1991).
30. S. A. A. Mansour, *J. Thermal Anal.* **46**, 263 (1996).
31. A. Y. Obaid, A. O. Alyoubi, A. A. Samarkandy, S. A. Al-Thabaiti, S. S. Al-Juaid, A. A. El-Bellihi, and El-H. M. Deifallah, *J. Therm. Anal. Cal.* **61**, 985 (2000).
32. J. Mu and D. D. Perlmutter, *Thermochimica Acta* **56**, 253 (1982).
33. S. A. A. Mansour, *J. Thermal Anal.* **45**, 1381 (1995).
34. E. G. King, A. D. Mah, and L. B. Pankratz, *INCRA Series on the Metallurgy of Copper*, 1973, USA.

TABLE I. List of experimental conditions and product compositions

Exp. No	Precursor	Co-solvent ^{a)} (Vol. fraction)	Furnace Temperature	Residence Time	Product (Major/Minor)
1		–	300 °C	2.3 sec	Cu ₂ O/Cu
2		10 %	300 °C	2.3 sec	Cu ₂ O/Cu
3	Copper	–	450 °C	2.0 sec	Cu/ Cu ₂ O
4	Acetate	10 %	450 °C	2.0 sec	Cu
5	(0.30 mol/L)	–	600 °C	1.8 sec	Cu
6		10 %	600 °C	1.8 sec	Cu
7		–	1000 °C	1.5 sec	Cu
8		10 %	1000 °C	1.5 sec	Cu

9		–	300 °C	2.3 sec	CuO
10		10 %	300 °C	2.3 sec	CuO
11	Copper	–	450 °C	2.0 sec	CuO/ Cu ₂ O
12	Nitrate	10 %	450 °C	2.0 sec	Cu/ Cu ₂ O
13	(0.30 mol/L)	–	600 °C	1.8 sec	Cu ₂ O/CuO
14		10 %	600 °C	1.8 sec	Cu
15		–	1000 °C	1.5 sec	Cu ₂ O/Cu
16		10 %	1000 °C	1.5 sec	Cu

17		–	600 °C	1.8 sec	NiO
18	Nickel	10 %	600 °C	1.8 sec	Ni/NiO
19	Nitrate	10 %	800 °C	1.7 sec	Ni/NiO
20	(0.30 mol/L)	10 %	900 °C	1.6 sec	Ni/NiO
21		30 %	900 °C	1.6 sec	Ni

^{a)} Ethanol was used as a co-solvent

TABLE II. Sources of oxygen in the spray pyrolysis reactor.

Source	O ₂ in the source (per mole)	Resulting O ₂ content in the reactor	
		Copper Acetate	Copper Nitrate
Carrier Gas (N ₂)	20 ppm ^{a)}	18.9 ppm	18.9 ppm
De-ionized H ₂ O	18 ppm ²⁵	1 ppm	1 ppm
Ethanol co-solvent	8 ppm ²⁶	< 0.1 ppm	< 0.1 ppm
Precursor	0.5 mole ²⁷	-	150 ppm
Total	-	19.9 ppm	169.9 ppm

^{a)} Reported from the vendor

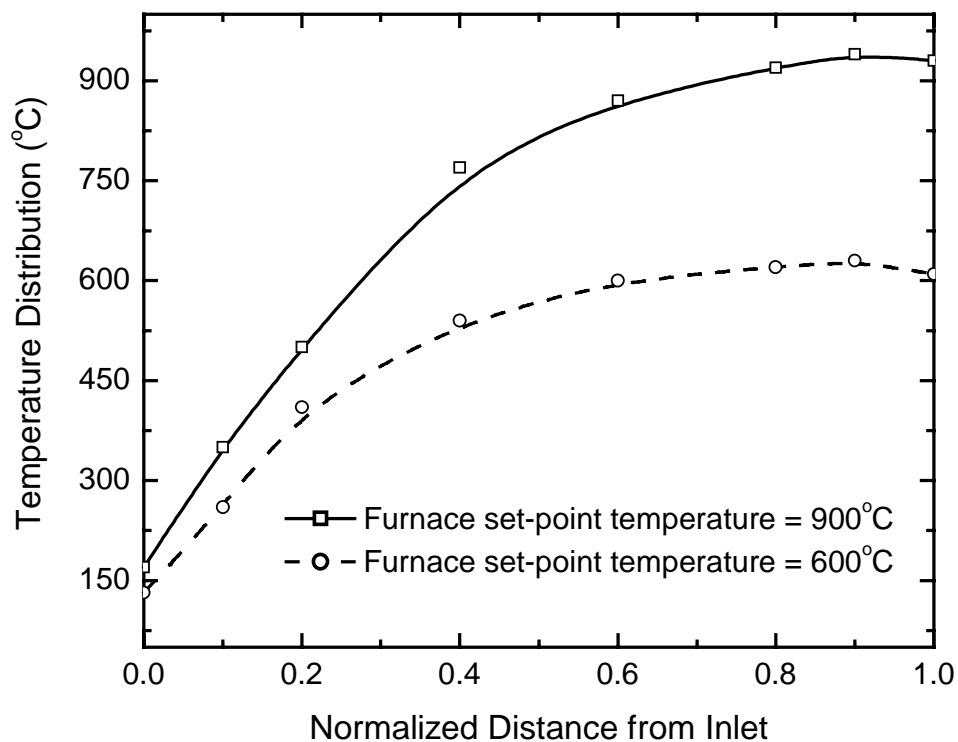


FIG. 1. Temperature distribution of the reactor inside. Reactor dimensions: 2.54 cm diameter and 76.2 cm length.

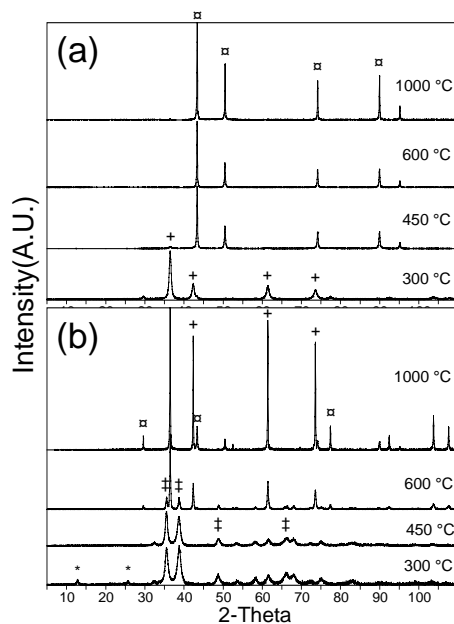


FIG. 2. X-ray diffraction patterns of copper powders obtained from (a) copper acetate and (b) copper nitrate 0.30 mol/L solutions in water at four different reaction temperatures: 300 °C, 450 °C, 600 °C, and 1000 °C (*: nitrate precursor, +: Cu_2O , ‡: CuO , ⌘: Cu).

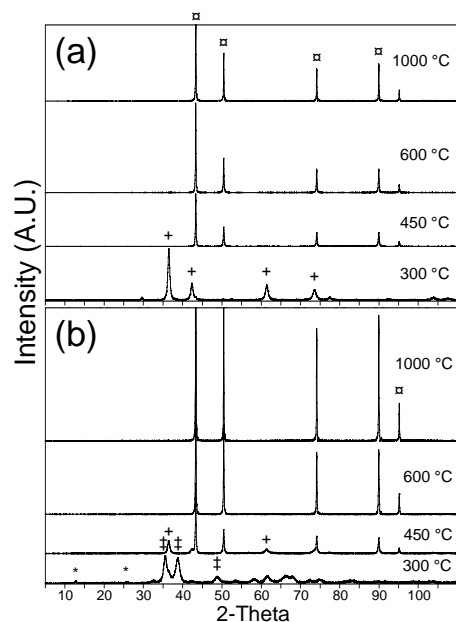


FIG. 3. X-ray diffraction patterns of copper powders obtained from (a) copper acetate and (b) copper nitrate 0.30 mol/L solutions with 10 volume percent ethanol in water at four different reaction temperatures: 300 °C, 450 °C, 600 °C, and 1000 °C (*: nitrate precursor, +: Cu_2O , ‡: CuO , ⌘: Cu).

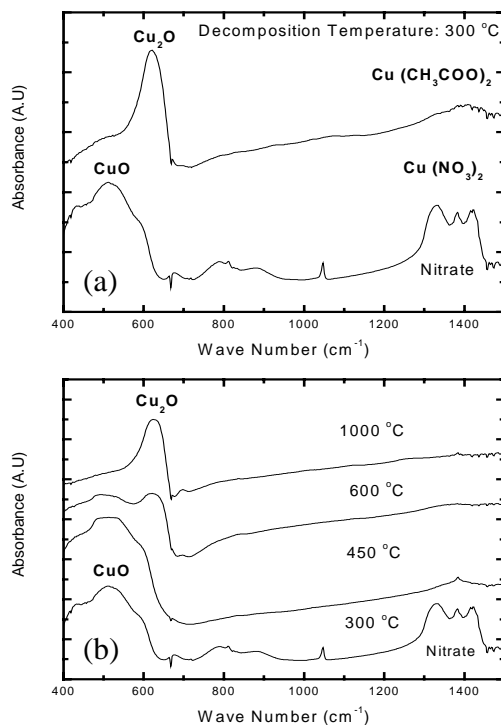


FIG. 4. Infrared spectroscopy results for copper powders. Figure (a) was measured for the powders produced from two different precursors at 300 °C, and figure (b) was measured for the powder produced from copper nitrate at four different temperatures.

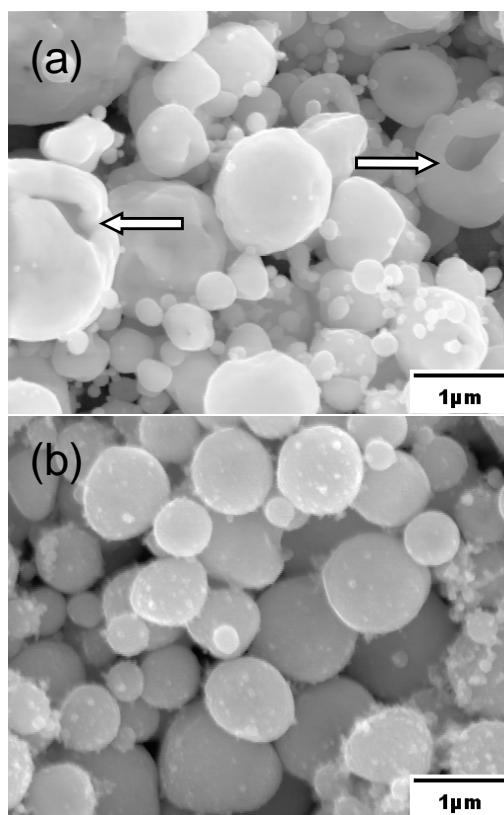


FIG. 5. SEM images of copper powders produced at (a) 600 °C and (b) 1000 °C from copper nitrate precursor with 10 % volume fraction of ethanol. Arrows indicate hollow particles.

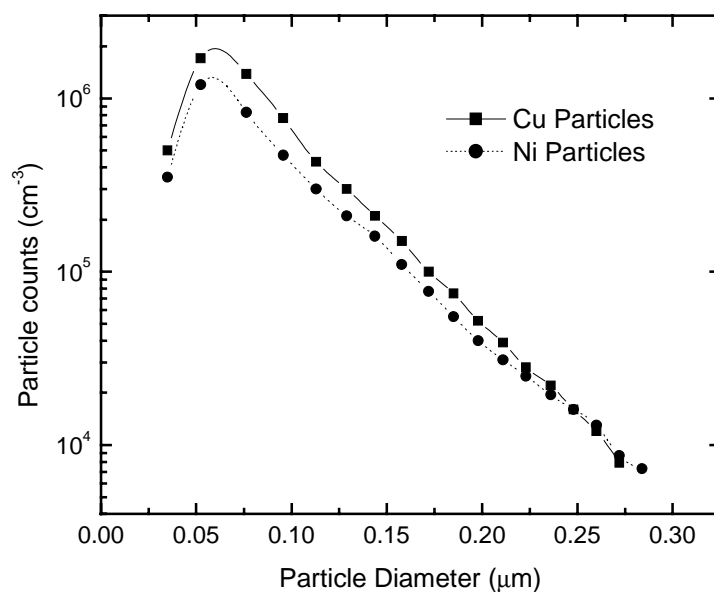


FIG. 6. Examples of the size distribution for the copper and nickel particles produced at 900 °C from copper nitrate and nickel nitrate 0.30 mol/L solutions.

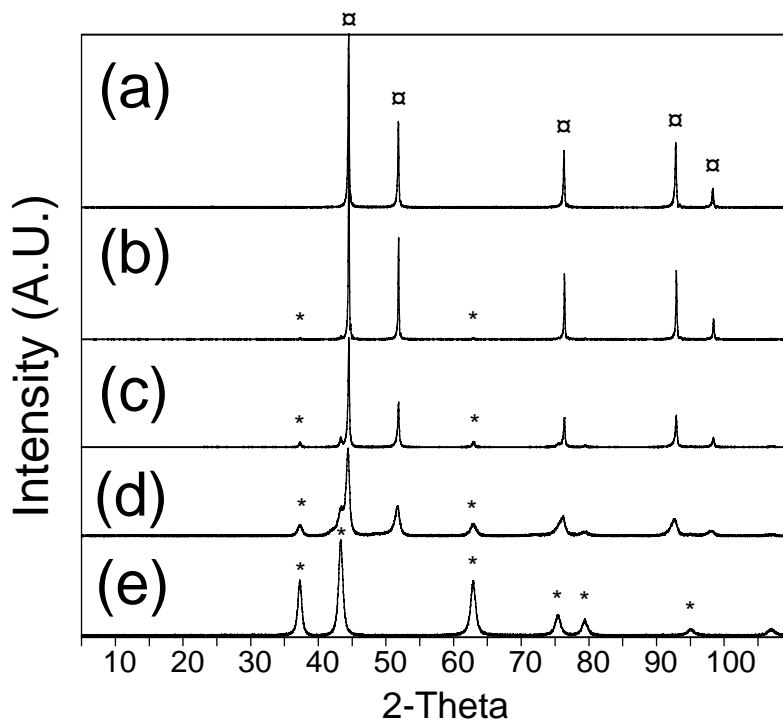


FIG. 7. X-ray diffraction patterns of nickel powder from nickel nitrate 0.30 mol/L solutions (a) at 900 °C with 30 volume percent ethanol in water, (b) at 900 °C and (c) at 800 °C with 10 volume percent ethanol in water, (d) at 600 °C with 10 volume percent ethanol in water, and (e) at 600 °C in water (*: NiO, □: Ni).

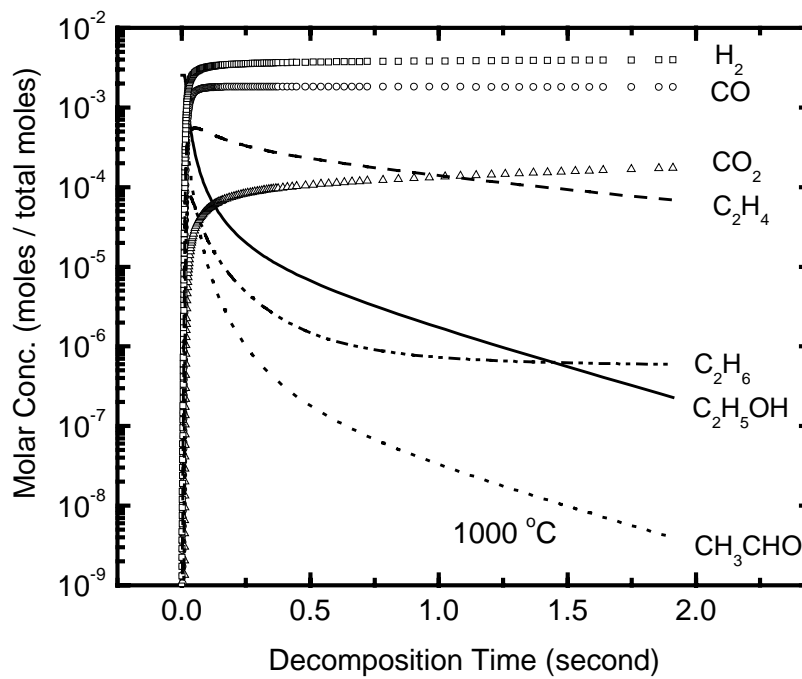


FIG. 8. Ethanol decomposition products at 1000 °C without oxygen.

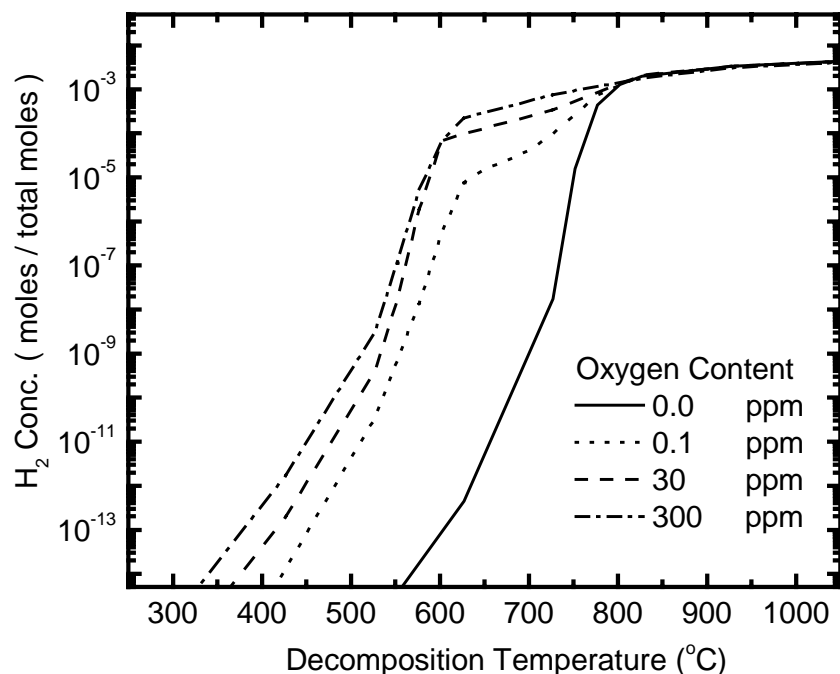


FIG. 9. Hydrogen concentration resulting from ethanol decomposition as a function of decomposition temperature for different oxygen concentrations at 1.5-second residence time (initial gas composition: $N_2 = 0.938$, $H_2O = 0.0586$, $C_2H_5OH = 0.00255$).

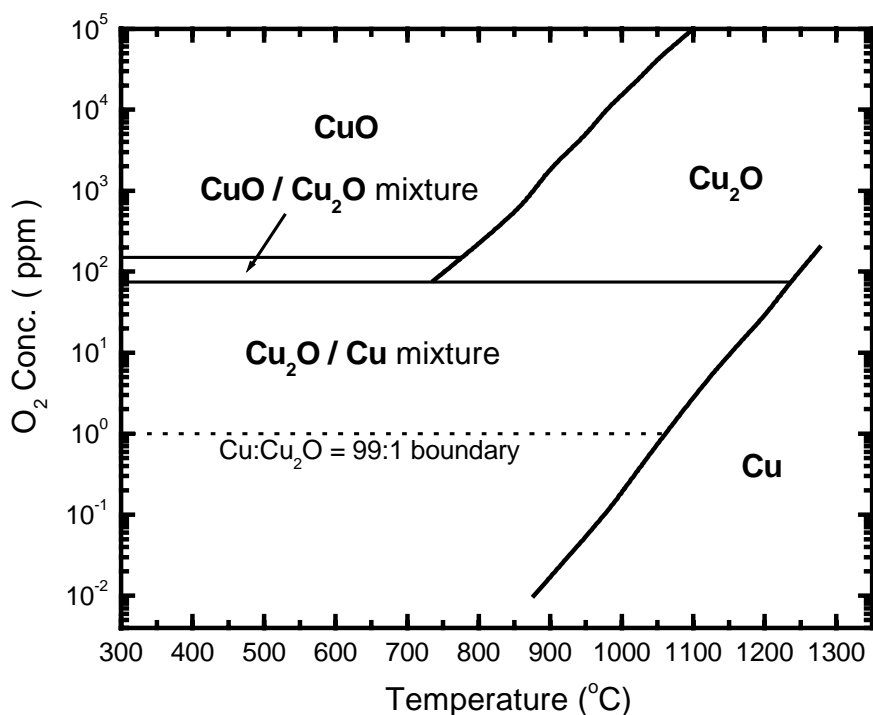


FIG. 10. Equilibrium phase diagram of the copper-oxygen system.